第43卷 第2期
2021年3月

地 球 科 学 与 环 境 学 报
Journal of Earth Sciences and Environment

Vol. 43 No. 2
Mar. 2021

张贵山,邱红信,彭 仁,等.扬子板块西缘攀西地区白草矿区黄铁矿标型元素特征及其指示意义[J].地球科学与环境学报,2021,43(2):262-275.
ZHANG Gui-shan,QIU Hong-xin,PENG Ren,et al. Characteristics of Pyrite Typomorphic Elements in Baicao Mining Area of Panzhihua-Xichang Region,the Western Margin of Yangtze Plate,China and Their Indication[J]. Journal of Earth Sciences and Environment,2021,43(2):262-275.

DOI:10.19814/j.jese.2020.09002

·庆祝长安大学建校七十周年专辑·

扬子板块西缘攀西地区白草矿区黄铁矿标型元素特征及其指示意义

张贵山[1,2],邱红信[1],彭 仁[1],孟乾坤[1],温汉捷[1,3],李石磊[4]

(1. 长安大学 地球科学与资源学院,陕西 西安 710054;2. 自然资源部岩浆作用成矿与找矿重点实验室,陕西 西安 710054;3. 中国科学院地球化学研究所 矿床地球化学国家重点实验室,贵州 贵阳 550081;4. 四川省川威集团矿业总公司,四川 成都 610059)

摘 要:黄铁矿是重要的金属硫化物矿物,在多种矿床中均有产出,其标型特征对矿床成因、矿体空间分布等具有重要的指示意义。以扬子板块西缘攀西地区白草矿区黄铁矿为研究对象,利用矿相学、电子探针等分析方法来对比研究浸染状、致密块状、斑杂状、网脉状矿石中黄铁矿的标型元素特征。结果表明:白草矿区黄铁矿 Fe、S 平均含量(质量分数,下同)分别为 46.030%、52.815%,介于岩浆成因与热液成因之间,根据矿石特征,黄铁矿以岩浆成因为主,并有少量热液作用参与;将白草矿区黄铁矿 δFe-δS 特征与金川等典型铜镍硫化物矿床黄铁矿对比,表明白草矿区黄铁矿为典型的岩浆熔离型;由于存在钒钛磁铁矿,Co/Ni 值多小于 5,说明钒钛磁铁矿与硫化物存在共生关系;岩浆内生成因黄铁矿 S/Se 值小于 15 000,白草矿区黄铁矿 S/Se 值为 812~10 466,显示白草矿区黄铁矿为岩浆内生成因;Se/Te 值随温度降低而升高,显示上述 4 类矿石黄铁矿结晶顺序为浸染状矿石→致密块状矿石→斑杂状矿石→网脉状矿石;原始地幔标准化主量、微量元素蛛网图显示白草矿区黄铁矿兼具岩浆成因与热液成因。综上所述,攀西地区白草矿区黄铁矿成因主要以岩浆熔离作用为主,并含有少量热液作用。

关键词:地球化学;黄铁矿;电子探针;标型元素;岩浆熔离作用;热液作用;成矿机制;扬子板块西缘
中图分类号:P571;P595 **文献标志码**:A **文章编号**:1672-6561(2021)02-0262-14

Characteristics of Pyrite Typomorphic Elements in Baicao Mining Area of Panzhihua-Xichang Region, the Western Margin of Yangtze Plate, China and Their Indication

ZHANG Gui-shan[1,2], QIU Hong-xin[1], PENG Ren[1], MENG Qian-kun[1], WEN Han-jie[1,3], LI Shi-lei[4]

(1. School of Earth Science and Resources, Chang'an University, Xi'an 710054, Shaanxi, China; 2. Key Laboratory for the Study of Focused Magmatism and Giant Ore Deposits of Ministry of Natural Resources, Xi'an 710054, Shaanxi, China; 3. State Key Laboratory of Ore Deposit Geochemistry, Institute of

收稿日期:2020-09-01;修回日期:2020-10-14 投稿网址:http://jese.chd.edu.cn/
基金项目:国家自然科学基金项目(41073027);中央高校基本科研业务费专项资金项目(310827172003);
陕西省自然科学基础研究计划项目(2019JM-161);财通矿山新兴关键矿产资源综合研究项目(030216190040)
作者简介:张贵山(1971-),男,黑龙江庆安人,长安大学副教授,理学博士,E-mail:zygszh@chd.edu.cn。

Geochemistry, Chinese Academy of Sciences, Guiyang 550081, Guizhou, China; 4. Mining Corporation of Sichuan Province Tranvic Group, Chengdu 610059, Sichuan, China)

Abstract: Pyrite is an important metal sulfide mineral, which occurs in many kinds of deposits. Its typomorphic characteristics are of great significance to the genesis of deposit and the spatial distribution of ore bodies. Taking pyrite in Baicao mining area of Panzhihua-Xichang region, the western margin of Yangtze plate as the research object, the typomorphic element characteristics of pyrite in four kinds of ores, such as disseminated, dense massive, taxitic and net vein, were comparatively studied by analytical methods of mineralography and electron probe micro-analyzer (EPMA). The results show that the average contents of Fe and S in pyrite are 46.030% and 52.815%, respectively, which are between magmatic and hydrothermal origins; according to ore characteristics, pyrite is mainly of magmatic origin, and a small amount of hydrothermal process also participate in the formation of pyrite; compared the δFe-δS characteristics of pyrite in Baicao mining area with those in Jinchuan and other typical Cu-Ni sulfide deposits, it is proved that the sulfide minerals in Baicao mining area are typical magmatic liquation type; the ratio of Co/Ni is less than 5 due to the existence of V-Ti magnetite, which indicates the symbiotic relationship between V-Ti magnetite and sulfide; the ratio of S/Se is 812—10 466, which is less than that of magmatic endogenetic pyrite (15 000), indicating that pyrite is of magmatic endogenetic origin; the ratio of Se/Te increases with the decrease of temperature, indicating that the crystallization order of pyrite is disseminated ore→dense massive ore→taxitic ore→net vein ore; the primitive mantle-normalized major and trace elements spider diagram shows that pyrite in Baicao mining area has both magmatic and hydrothermal origins. Based on the above typomorphic element characteristics, it is considered that pyrite in Baicao mining area is mainly caused by magmatic liquated mineralization and contains a small amount of hydrothermal action.

Key words: geochemistry; pyrite; electron microprobe; typomorphic element; magmatic liquated mineralization; hydrothermal action; metallization mechanism; the western margin of Yangtze plate

0　引　言

黄铁矿是重要的金属硫化物矿物[1-10]。利用黄铁矿标型特征来探讨矿床成因和预测矿体分布已被广泛应用于实际工作中。标型元素是黄铁矿最主要的标型特征之一,包含了大量成矿信息,在黄铁矿标型特征中具有无法替代的地位[11]。因此,众多学者对黄铁矿标型元素特征进行了相关研究,积累了大量资料[12-15]。

攀西地区是中国主要钒钛磁铁矿矿集区,但也有独立的铜镍硫化物矿床产出,集中形成于263～250 Ma[16],这些矿床[17-31]与钒钛磁铁矿形成时间[32]基本一致。前人对铜镍硫化物矿床成因做了大量研究,但关于硫化物的形成机制与硫源等还存在不确定性和争议,如地幔硫和地壳硫混染之争[33]、地壳硫混染机制[34-35]等。攀西地区除了独立铜镍硫化物矿床之外,还发育富钴硫化物矿床,常以与钒钛磁铁矿共伴生或独立富钴硫化物等形式产出。赋存在钒钛磁铁矿矿床中的富钴硫化物成因机制研究还比较薄弱,选择攀西地区富钴硫化物作为研究对象,系统讨论富钴硫化物矿床成因和硫化物形成机制,为该地区金属硫化物矿床成矿理论提供证据,对丰富峨眉山地幔柱成矿理论具有重要意义[36]。

课题组在攀西地区白草钒钛磁铁矿矿区野外地质调查时发现,矿区内发育大量富钴硫化物矿物,呈浸染状、致密块状、斑杂状和网脉状产出。基于此,本文将通过对白草矿区4类矿石中黄铁矿标型元素特征的研究,来讨论硫化物的成因及其与钒钛磁铁矿的关系,为本区金属硫化物矿床成矿作用的研究提供借鉴。

1　地质概况

1.1　区域地质特征

攀西地区位于扬子板块西缘,发育中条期和晋宁期形成的SN向深大断裂和EW向次级断裂。深

大断裂自西向东依次为程海深大断裂带、攀枝花深大断裂带、昔格达—元谋深大断裂带、安宁河深大断裂带，在时空上控制了基性—超基性侵入体(富含钒钛磁铁矿和铜镍硫化物)的分布[37]。地层出露较为完整，主要由结晶基底和盖层组成，基底为前震旦系杂岩，混合岩化作用强烈，盖层为震旦系到第四系地层[38]。岩浆岩具有规模大、分布广的特点，岩浆作用可分为元古、加里东—华力西—印支、燕山—喜山3个旋回。元古旋回主要出露在康滇地轴，主要是岩体侵位于康定群变质岩中，以花岗片麻岩为主，原岩为花岗闪长岩。加里东—华力西—印支旋回由于安宁河地体与盐边地体合并产生挤压作用，使地幔部分熔融，产生玄武岩岩浆和碱性岩浆，形成了基性—超基性岩体和碱性岩体，二叠纪末期岩浆活动达到顶峰，产生攀西岩浆活动标志性岩石——峨眉山玄武岩。燕山—喜山旋回岩浆岩主要为燕山—喜山陆内造山运动产物，岩石组合分为地幔混源型富碱浅成—超浅成侵入岩组合、幔源型碱性侵入岩组合、壳源型花岗岩组合三大类[39-40]。

白草矿区地层出露简单，仅有前震旦系会理群和第四系残坡积地层出露。岩浆岩分布广泛，玄武岩和正长岩大面积分布，正长岩呈岩株分布于矿区西部，辉长岩脉、辉绿岩脉及少量正长岩脉主要呈NE向侵位于玄武岩中，面积相对较小的橄辉岩呈NW向分布于玄武岩中，钒钛磁铁矿矿体近SN向分布于含矿辉长岩岩体内。构造较为发育，受区域上SN向昔格达—元谋深大断裂带、安宁河深大断裂带控制明显[41]，并有NE向和EW向次一级断裂发育(图1)。

1.2　金属硫化物矿石特征

白草矿区富钴硫化物矿石主要有4种类型：浸染状、致密块状、斑杂状和网脉状。浸染状矿石中金属硫化物主要呈星点状分布于钒钛磁铁矿的中部或边缘，体积分数约为4%，主要矿物组合为黄铁矿、黄铜矿、磁黄铁矿，比例为3∶1∶96[图2(a)]；致密块状矿石产于致密块状钒钛磁铁矿矿体、辉长岩或辉石岩的下部，产状与致密块状钒钛磁铁矿矿体基本一致，硫化物体积分数大于75%，主要矿物组合为黄铁矿、黄铜矿、磁黄铁矿，比例为2∶5∶93[图2(b)]；网脉状矿石中金属硫化物体积分数约为8.79%，产于辉石岩和辉绿岩裂隙中，主要矿物组合为黄铁矿、黄铜矿、磁黄铁矿，比例为1∶1∶98[图2(c)]；斑杂状矿石中金属硫化物体积分数约为15%，产出于正长岩-碳酸岩等碱性杂岩与围岩接触处，主要矿物组合为黄铁矿、黄铜矿、磁黄铁矿，比例为5∶10∶85[图2(d)]。

白草矿区硫化物矿物主要为黄铁矿、磁黄铁矿、黄铜矿及少量紫硫镍矿。黄铁矿主要呈他形粒状，粒径为0.1～1.0 mm，多与磁黄铁矿、黄铜矿共生；磁黄铁矿多为半自形—他形粒状结构，以他形粒状结构为主，粒径约为0.5 mm，常与黄铁矿、黄铜矿共生；黄铜矿一般为他形粒状，粒径较细，一般为0.1～0.2 mm，氧化色为锖色；紫硫镍矿发育于黄铁矿中，主要呈他形粒状产出，粒径为0.1～0.3 mm(图3)。

2　样品采集与分析方法

2.1　样品采集

本次研究共采集样品15件，其中，致密块状矿石样品3件、浸染状矿石样品8件、斑杂状矿石样品2件、网脉状矿石样品2件，采样位置见图1。浸染状矿石采自钒钛磁铁矿中部，矿石以钒钛磁铁矿为主，硫化物含量较少；致密块状矿石采自钒钛磁铁矿矿体下部，矿石以硫化物矿物为主；斑杂状矿石样品采自正长岩与围岩接触部位，以巨晶辉石和巨晶黑云母为主；网脉状矿石样品采自辉绿岩中，硫化物以网脉状分布于岩石中。

2.2　分析方法

将野外采集样品磨制成探针片，首先在矿相显微镜下观察并圈定待测位置，然后在电子探针分析仪上进行测试分析，测试单位为东华理工大学核资源与环境国家重点实验室，仪器型号为JXA-8530。测试条件包括：加速电压为30 kV，束电流为20 nA，束斑直径为40 nm，分析精度为0.01%。黄铁矿电子探针分析结果见表1。

3　结果分析与讨论

不同物理化学条件下形成的黄铁矿化学组成存在微小差异，利用电子探针等现代高精度测试仪器可分辨这些差异，据此能够发现大量成矿地质作用信息用于进一步探讨矿物成因[42-43]。

3.1　Fe和S特征

不同成因的黄铁矿中Fe和S含量(质量分数，下同)存在差异，如表2所示。攀西地区白草矿区致密块状矿石黄铁矿S含量为52.001%～52.958%，平均值为52.446%，Fe含量则为45.898%～47.304%，平均值为46.728%；浸染状矿石黄铁矿S含量为52.068%～54.458%，平均值为53.112%，

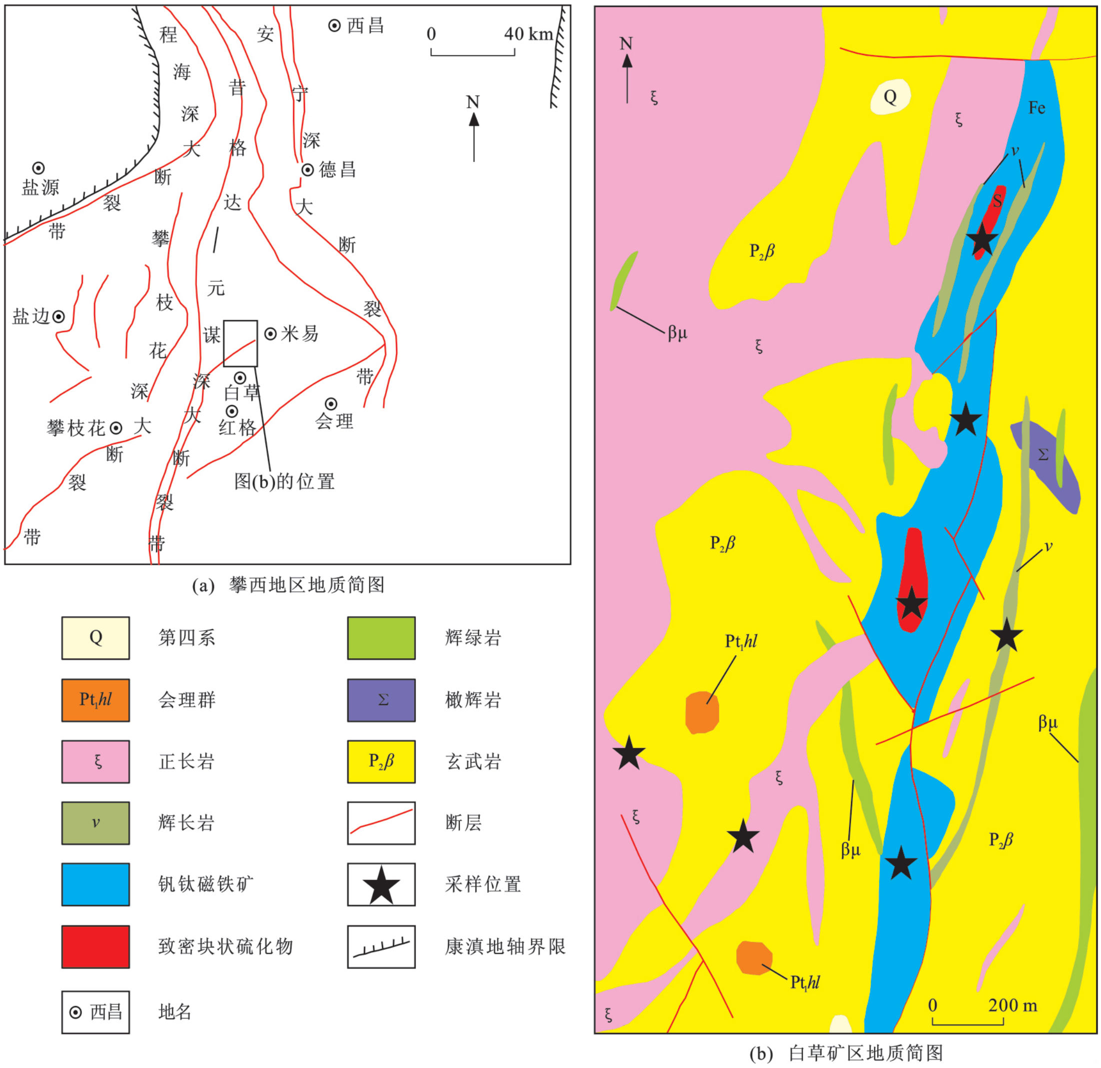

底图分别引自文献[44]和[45]

图 1　扬子板块西缘攀西地区白草矿区地质简图

Fig. 1　Geological Sketch Maps of Baicao Mining Area in Panzhihua-Xichang Region, the Western Margin of Yangtze Plate

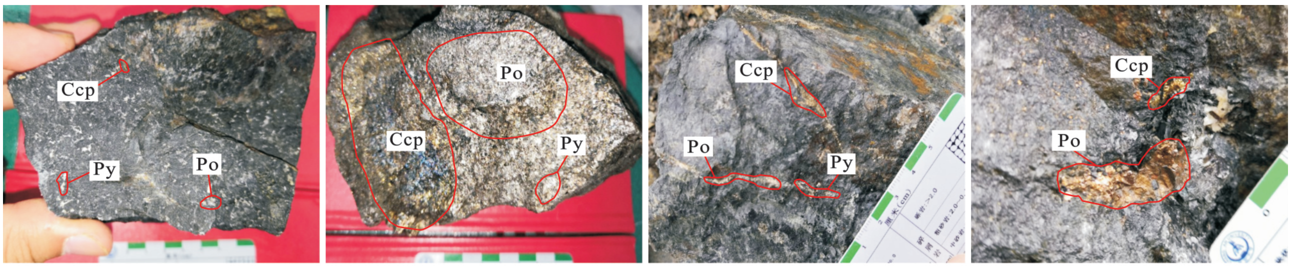

(a) 浸染状矿石　(b) 致密块状矿石　(c) 网脉状矿石　(d) 斑杂状矿石

Po 为磁黄铁矿；Py 为黄铁矿；Ccp 为黄铜矿

图 2　富钴硫化物矿石手标本照片

Fig. 2　Hand Specimen Photos of Cobalt-rich Sulfide Ores

Fe 含量则为 42.388%～46.846%，平均值为 45.385%；斑杂状矿石黄铁矿 S 含量为52.108%～53.764%，平均值为 52.812%，Fe 含量则为 44.426%～47.360%，平均值为 46.337%；网脉状矿石黄铁矿 S 含量为 52.520%～52.624%，平均值为 52.572%，Fe 含量则为 43.261%～47.217%，平均值为45.239%。白草矿区 Fe、S 含量与表 2 中所列矿床略有差异，主要介于与超基性岩有关的矿床和热液成因矿床中黄铁矿的 Fe、S 含量之间。根据本区硫同位素数据（未发表），结合野外发现的网脉

表1　黄铁矿电子探针分析结果

Tab. 1　Electron Microprobe Analysis Results of Pyrite

矿石类型	样品编号	w(As)/%	w(Se)/%	w(S)/%	w(Fe)/%	w(Ag)/%	w(Cu)/%	w(Au)/%	w(Te)/%	w(Ni)/%	w(Co)/%	w_{total}/%	Co/Ni值	S/Se值	Se/Te值
致密块状	B4-1-1	—	—	52.133	46.124	—	0.025	0.040	0.001	1.168	—	99.491	—	—	—
	B4-1-5	—	—	52.958	46.555	—	0.008	0.033	0.018	0.668	0.153	100.393	0.229	—	—
	B4-1-9	—	0.005	52.330	45.898	—	—	0.050	0.018	1.119	—	99.420	—	10 466	0.278
	B21-1-7	—	—	52.834	47.304	—	—	—	—	0.169	0.183	100.490	1.083	—	—
	B21-1-8	0.020	0.007	52.643	46.856	—	0.019	—	—	0.203	0.186	99.934	0.916	7 520	—
	B21-1-12	0.061	0.018	52.514	47.139	0.035	0.014	—	—	0.086	0.126	99.993	1.465	2 917	—
	B21-1-19	—	—	52.402	47.138	0.015	—	0.013	—	0.160	0.203	99.931	1.269	—	—
	B38-1-9	—	—	52.196	46.954	—	—	0.063	—	0.243	0.224	99.680	0.922	—	—
	B38-1-10	0.001	0.019	52.001	46.585	0.022	—	0.023	—	0.243	0.244	99.138	1.004	2 737	—
浸染状	B25-1-4	—	0.048	53.248	46.394	0.005	0.094	—	0.009	0.205	0.269	100.272	1.312	1 109	5.333
	Y5-1-2	—	0.010	52.154	46.228	—	0.002	0.007	0.011	0.693	0.429	99.534	0.619	5 215	0.909
	Y5-1-6	—	0.047	52.068	46.686	0.007	—	0.020	0.028	0.500	0.287	99.643	0.574	1 108	1.679
	01-6	0.039	—	52.484	45.118	—	—	0.253	0.030	0.652	—	98.576	—	—	—
	5910-2	0.015	0.046	54.458	44.236	0.041	0.041	—	0.051	0.722	—	99.610	—	1 184	0.902
	5910-3	0.033	0.027	53.203	42.388	0.037	0.037	—	—	—	3.711	99.436	—	1 970	—
	5910-6	0.005	0.009	53.231	45.782	0.020	0.020	0.097	0.061	0.538	—	99.763	—	5 915	0.148
	62631-1	0.020	0.042	53.277	46.055	—	—	0.044	0.038	0.128	—	99.604	—	1 269	1.105
	782-6	0.003	0.016	52.452	45.040	0.011	0.011	0.158	0.056	0.881	—	98.628	—	3 278	0.286
	7824-4	0.007	—	52.526	46.846	—	—	—	0.038	0.049	—	99.466	—	—	—
	7824-5	—	—	53.781	45.816	—	—	—	0.058	0.073	—	99.728	—	—	—
	784-1	—	0.012	53.271	45.741	0.017	0.017	—	0.047	0.314	—	99.419	—	4 439	0.255
	784-3	—	—	54.298	43.676	0.002	0.002	—	—	0.173	—	98.151	—	—	—
斑杂状	B26-5-2	—	0.013	52.678	46.834	—	—	0.037	—	0.038	0.162	99.762	4.263	4 052	—
	B26-5-3	0.006	0.014	52.646	46.701	—	—	—	—	0.025	0.161	99.553	6.440	3 760	—
	B26-5-7	—	0.065	52.760	46.670	—	—	—	0.008	0.179	0.198	99.880	1.106	812	8.125
	B26-5-8	—	—	52.789	46.667	—	0.007	0.023	—	0.024	0.139	99.649	5.792	—	—
	B26-5-10	—	—	52.664	47.131	—	—	0.013	—	—	0.122	99.930	—	—	—
	B26-7-1	—	—	52.108	46.526	—	—	—	—	—	0.143	98.777	—	—	—
	B26-7-3	—	—	52.385	46.655	—	0.014	0.066	0.010	0.134	0.109	99.373	0.813	—	—
	B26-7-4	—	0.022	52.816	47.360	—	0.042	—	—	—	0.120	100.360	—	2401	—
	B26-7-5	—	0.016	52.721	46.980	—	—	—	0.009	—	0.123	99.849	—	3295	1.778
	B26-7-7	0.013	—	53.764	44.737	0.015	—	0.023	—	—	2.661	101.213	—	—	—
	B26-7-8	—	—	53.244	44.426	—	—	0.090	0.005	—	2.586	100.351	—	—	—
	B26-7-9	—	0.049	53.172	45.353	0.021	0.005	—	—	—	2.228	100.828	—	1085	—
网脉状	C2-3-2	—	—	52.520	47.217	0.021	0.048	0.037	—	0.187	0.105	100.135	0.561	—	—
	5719-9	0.054	0.010	52.624	43.261	0.011	0.011	—	0.006	—	2.710	98.687	—	5262	1.667

注：$w(\cdot)$为元素含量；w_{total}为主量元素总含量；“—”表示元素含量低于检测限。

状硫化物沿节理或裂隙穿插于钒钛磁铁矿矿体或辉长岩中的地质现象，可知网脉状硫化物为后期充填形成的，暗示白草矿区黄铁矿主要为岩浆型铜镍硫化物类型夹杂少量高温热液成因类型。

3.2　δFe-δS 特征

严育通等提出以 δFe 和 δS 进行黄铁矿主量元素标型特征分析[46]。δFe 和 δS 分别表示 Fe 和 S 含量偏离理论值的程度（Fe 含量理论值为46.55%，S 含量理论值为 53.45%），既表示质量偏离程度，也可以表示元素个数偏离程度。其表达式分别为

$$\delta(\mathrm{Fe})=\frac{100(w(\mathrm{Fe})-46.55\%)}{46.55} \tag{1}$$

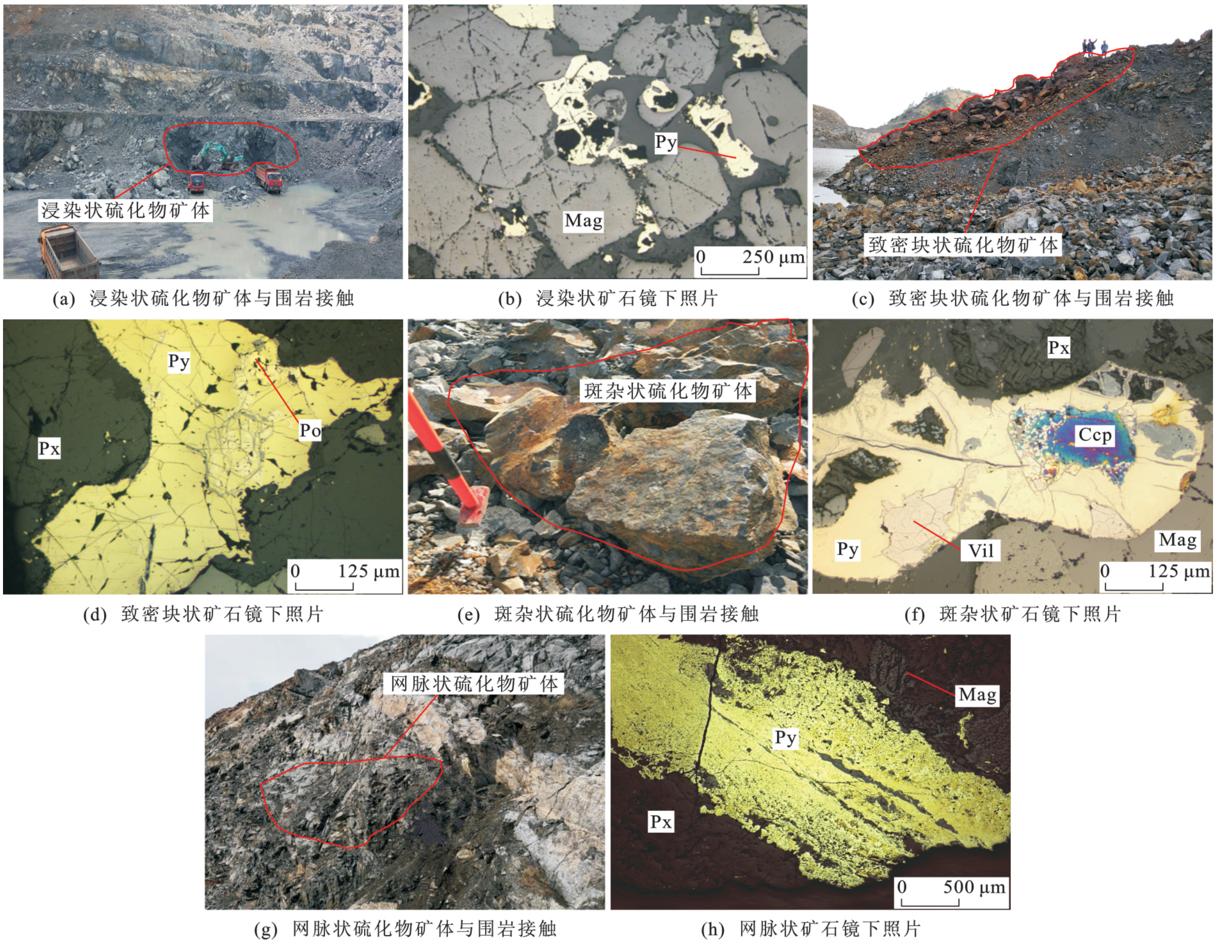

(a) 浸染状硫化物矿体与围岩接触　(b) 浸染状矿石镜下照片　(c) 致密块状硫化物矿体与围岩接触

(d) 致密块状矿石镜下照片　(e) 斑杂状硫化物矿体与围岩接触　(f) 斑杂状矿石镜下照片

(g) 网脉状硫化物矿体与围岩接触　(h) 网脉状矿石镜下照片

Mag 为磁铁矿;Vil 为紫硫镍矿;Px 为辉石

图 3　富钴硫化物矿石野外照片与镜下照片

Fig. 3　Outcrop Photos and Photomicrographs of Cobalt-rich Sulfide Ores

$$\delta(\mathrm{S})=\frac{100(w(\mathrm{S})-53.45\%)}{53.45} \qquad (2)$$

式中:$\delta(\mathrm{Fe})$为 δFe 值,$\delta(\mathrm{S})$为 δS 值。

将白草矿区黄铁矿与世界著名岩浆铜镍硫化物矿床黄铁矿利用式(1)、(2)进行计算,并投点在δFe-δS 特征图解(图 4)上。从图 4 可以看出,δFe、δS 值均较大,部分 δFe 值已经超过 5%,数据点主要集中于第三、四象限。白草矿区黄铁矿与南非 Bushveld[47],加拿大 Sudbury[48],中国金川[49]、夏日哈木[50]、红旗岭[51-52]、喀拉通克[53-54]、煎茶岭[55]等矿床黄铁矿具有相似的 δFe、δS 值,表明这些地区黄铁矿具有相似的形成条件。

3.3　Co 和 Ni 特征

Fe、Co、Ni 化学性质相似,但也存在微小差异,亲氧性从大到小依次为 Fe、Co、Ni,亲硫性则相反。黄铁矿中 Co、Ni 常以类质同象替换 Fe 的形式存在。由于 Co 与 Fe 的相似性强于 Ni 与 Fe,所以 Ni 含量越高,Co/Ni 值越低,指示黄铁矿杂质含量越高,矿物结晶越快[56]。因此,Co/Ni 值是区分不同矿床成因的有效指标。岩浆铜镍硫化物矿床中黄铁矿 Co/Ni 值约为 1 200,岩浆熔离型钒钛磁铁矿矿床中约为 0.09,沉积成因矿床中约为 0.30,岩浆热液成因矿床中约为 3.00,变质热液成因矿床中约为 0.50[57-62]。

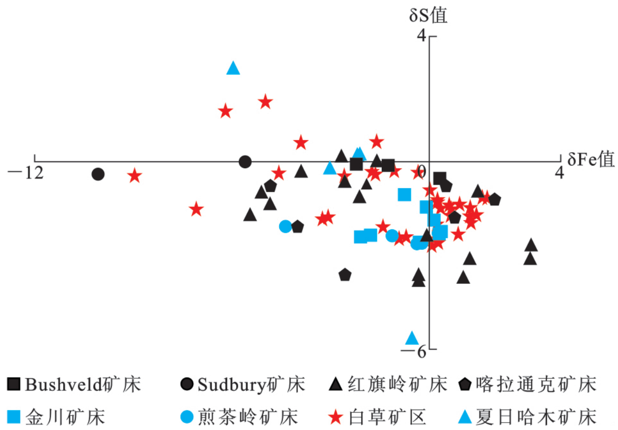

图 4　黄铁矿 δFe-δS 特征图解

Fig. 4　Characteristic Diagram of δFe-δS of Pyrite

表2 不同成因类型矿床中黄铁矿Fe、S含量特征

Tab. 2 Characteristics of Fe and S Contents of Pyrite in Different Genetic Types of Ore Deposits

矿床类型	w(Fe)/%	w(S)/%	硫类型
沉积成因矿床	46.16	53.84	多硫型
黄铁矿型铜矿床	47.76	52.24	亏硫型
多金属硫化物矿床	47.76	52.24	亏硫型
斑岩型铜矿床	47.67	52.33	亏硫型
热液成因矿床	45.08	52.50	亏硫型
与超基性岩有关的矿床	46.76	53.24	亏硫型
与火山作用有关的低温热液矿床	46.60	53.39	亏硫型
黄铁矿理论值	46.55	53.45	
白草矿区	46.03	52.81	亏硫型

注:白草矿区数据为本文实测;其他数据引自文献[63]和[64]。

白草矿区致密块状矿石黄铁矿Co/Ni值为0.229～1.465,平均值为0.984;浸染状矿石黄铁矿Co/Ni值为0.574～1.312,平均值为0.835;斑杂状矿石黄铁矿Co/Ni值为0.813～6.440,平均值为3.683;网脉状矿石黄铁矿Co/Ni值为0.561。浸染状矿石、致密块状矿石、网脉状矿石黄铁矿Co/Ni值接近于岩浆熔离型钒钛磁铁矿矿床,斑杂状矿石更接近岩浆热液成因矿床。将4类矿石黄铁矿Co/Ni值投影于Co-Ni图解[图5(a)]中,多数样品Co/Ni值为0.5～2.0,落在岩浆成因范围,少数样品落在热液成因附近,说明白草矿区同时存在岩浆作用和热液作用。这一点在Co/Ni-Co图解[图5(b)]中也得到了较好的证明。

3.4 S、Se和Te特征

Se、Te与S地球化学性质相似,在硫化物成矿过程中经常参与矿化,因此,Se、Te是黄铁矿标型元素之一。Se、Te由于化学性质相似,经常被视为一个地球化学元素对[65]。Se、Te元素丰度分布如表3所示。Se、Te在地壳中以分散状态存在,绝大多数分散到硫化物矿物晶格中,少数形成独立矿物。Se、Te在岩浆期后热液阶段富集,以分散状态分布于硫化物中或形成独立矿物。S/Se值可用来判断矿物的生成环境,沉积成因矿床硫化物S/Se值为几万到十几万,岩浆内生作用形成的硫化物S/Se值小于15 000,热液成因矿床硫化物S/Se值为10 000～28 000,层控矿床黄铁矿S/Se值为176 000～334 000,同生沉积型矿床黄铁矿S/Se值大于30 000[66-68]。Se与S化学性质相似性比Te与S大,当温度变化且发生类质同象时,Se比Te更容易替代S,使Se/Te值发生剧烈变化,因此,Se/Te值可以反映成矿温度的变化。当温度降低时,Se更易进入矿物晶格,使Se/Te值变大[11]。

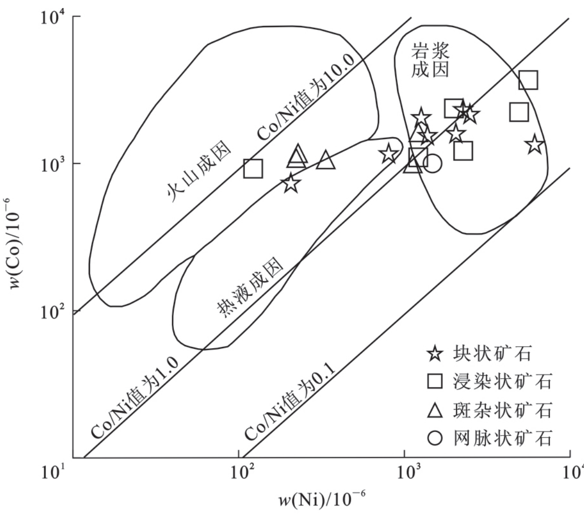

(a) Co-Ni图解

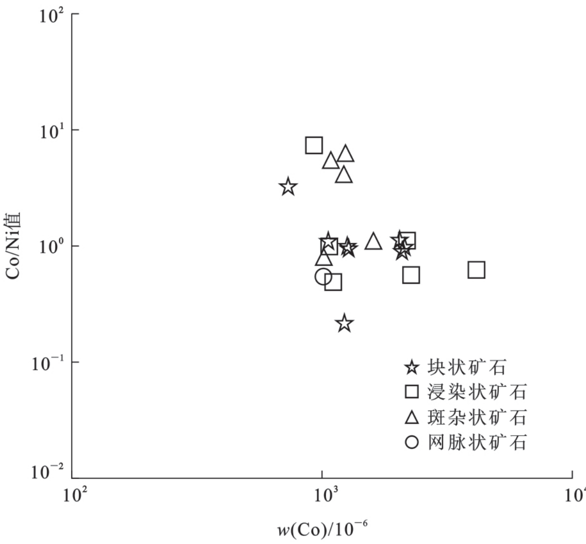

(b) Co/Ni-Co图解

图(a)引自文献[58]、[69]和[70]

图5 黄铁矿Co-Ni图解和Co/Ni-Co图解

Fig. 5 Diagrams of Co-Ni and Co/Ni-Co of Pyrite

白草矿区黄铁矿S/Se值为812～10 466,平均值为3 529,大部分为1 000～7 600,显示黄铁矿为岩浆内生成因。致密块状矿石黄铁矿Se/Te值为0.278,浸染状矿石为0.148～5.333,平均值为1.327,斑杂状矿石为1.778～8.125,平均值为4.952,网脉状矿石为1.667。从浸染状矿石到斑杂状矿石,黄铁矿Se/Te值逐渐变大,表明其结晶温度逐渐变低。网脉状矿石黄铁矿Se/Te值变小,可能是本次所测数据较少引起的。野外观察发现网脉状硫化物沿节理或裂隙发育在辉石岩、钒钛磁铁矿矿体中,说明网脉状硫化物为热液产物。因此,白草矿区4类矿石中黄铁矿结晶顺序为浸染状矿石→致密块状矿石→斑杂状矿石→网脉状矿石。

表 3　Se、Te 元素丰度分布

Tab. 3　Distribution of Element Abundance of Se and Te

元素	地球	上地幔	下地幔	地核	地壳	中国陆壳	陆壳
Se	13.000×10^{-6}	0.050×10^{-6}	0.050×10^{-6}	40.000×10^{-6}	0.080×10^{-6}	0.074×10^{-6}	0.080×10^{-6}
Te		0.001×10^{-6}	0.001×10^{-6}	0.520×10^{-6}	5.5×10^{-10}		4.5×10^{-10}
元素	球粒陨石	超基性岩	基性岩	中性岩	酸性岩	沉积岩	洋壳
Se	1×10^{-9}	5×10^{-12}	5×10^{-12}	5×10^{-12}	5×10^{-12}	6×10^{-11}	5.6×10^{-8}
Te	5×10^{-11}	1×10^{-13}	1×10^{-13}	1×10^{-13}	1×10^{-13}	1×10^{-12}	9.5×10^{-10}

注：数据引自文献[71]。

3.5　主量、微量元素特征

本文通过统计岩浆型金川[49]、红旗岭[51]矿床和热液型科洛[72]、多不杂[73]矿床中黄铁矿的主量、微量元素数据，绘制了黄铁矿的原始地幔标准化主量、微量元素蛛网图(图 6)，并与白草矿区黄铁矿进行对比研究。网脉状矿石黄铁矿主量、微量元素特征与科洛矿床相似，说明其为热液成因；浸染状、块状、斑杂状矿石黄铁矿主量、微量元素特征与红旗岭矿床相似，说明其为岩浆成因。因此，白草矿区黄铁矿以岩浆成因为主，夹少量热液成因。

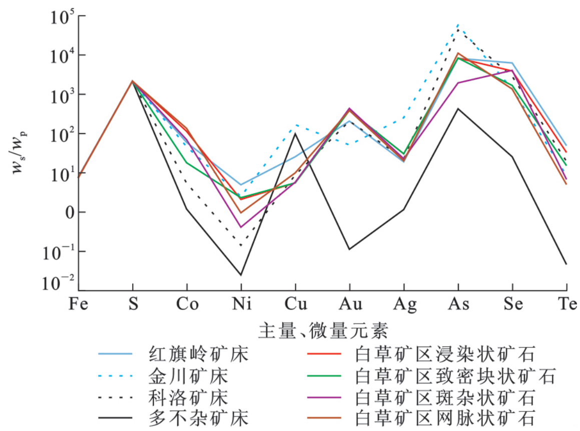

w_s 为样品含量；w_p 为原始地幔含量；原始地幔标准化数据引自文献[74]；白草矿区不同矿石黄铁矿数据均为平均值

图 6　黄铁矿原始地幔标准化主量、微量元素蛛网图

Fig. 6　Primitive Mantle-normalized Major and Trace Elements Spider Diagram of Pyrites

3.6　成矿机制

白草矿区成矿初期基性—超基性岩浆发生熔离作用，产生钒钛磁铁矿浆和硫化物矿浆[75-81]。硫化物矿浆密度较大，在重力作用下，硫化物矿浆向下富集并结晶形成致密块状矿石[82-86]。钒钛磁铁矿结晶温度高于硫化物，位于上部的矿浆先结晶形成钒钛磁铁矿，残留的硫化物熔体充填在磁铁矿、钛铁矿和辉石等矿物中间，造成白草矿区富钴浸染状矿石中硫化物含量偏低。浸染状矿石分布于致密块状矿石上部，产状相同，两者的 Se/Te 值相差不大，说明致密块状矿石结晶稍晚于浸染状矿石。正长岩岩浆与围岩发生交代作用形成斑杂状矿石[87]，该类矿石中发育绿泥石、绿帘石等典型的接触交代蚀变矿物，说明斑杂状矿石硫化物为接触交代作用成因且晚于致密块状矿石。最后，岩浆期后热液沿构造裂隙贯入成矿，因此，在野外可见网脉状硫化物多沿节理或钒钛磁铁矿矿体与围岩裂隙发育。

4　结　语

(1)扬子板块西缘攀西地区白草矿区黄铁矿的 Fe、S、δFe-δS 特征及原始地幔标准化主量、微量元素蛛网图表明，造成白草矿区黄铁矿富集、结晶的主要因素为岩浆熔离作用，岩浆热液也参加了部分成矿作用。

(2)白草矿区黄铁矿 Co-Ni 特征表明黄铁矿与钒钛磁铁矿共生；S/Se 值小于 15 000，表明黄铁矿为岩浆内生成因；黄铁矿 Se/Te 值按浸染状矿石、致密块状矿石、斑杂状矿石顺序逐渐变高，说明其结晶温度逐渐变低。

(3)结合黄铁矿标型元素特征及其野外产出特征，白草矿区 4 类矿石中黄铁矿以岩浆熔离作用为主，含少量岩浆期后热液作用，结晶顺序为浸染状矿石→致密块状矿石→斑杂状矿石→网脉状矿石。

枝繁叶茂承先启后七十载春风育桃李，天高地阔继往开来新世纪振翅展宏图！谨以此文庆祝长安大学七十岁生日快乐。七十年春华秋实，长安大学已是桃李满天下，一代代长大人秉承“弘毅明德、笃学创新”的校训，为国家建设和社会发展做出了卓越的贡献。七十年的岁月变迁，长大走出了自己的康庄大道，并在多个领域具有了强劲的竞争力。未来的时光里，相信长大会不负韶华，更上一层楼！

参 考 文 献：

References：

[1]　汤中立，闫海卿，焦建刚，等．中国小岩体镍铜(铂族)矿床的区域成矿规律[J]．地学前缘，2007，14(5)：92-

103.
TANG Zhong-li, YAN Hai-qing, JIAO Jian-gang, et al. Regional Metallogenic Controls of Small-intrusion-hosted Ni-Cu(PGE) Ore Deposits in China[J]. Earth Science Frontiers, 2007, 14(5): 92-103.

[2] **汤中立,焦建刚,闫海卿,等.小岩体成(大)矿理论体系**[J].**中国工程科学**,2015,17(2):4-18.
TANG Zhong-li, JIAO Jian-gang, YAN Hai-qing, et al. Theoretical System for (Large) Deposit Formed by Smaller Intrusion[J]. Engineering Science, 2015, 17(2): 4-18.

[3] **汤中立,钱壮志,姜常义,等.岩浆硫化物矿床勘查研究的趋势与小岩体成矿系统**[J].**地球科学与环境学报**,2011,33(1):1-9.
TANG Zhong-li, QIAN Zhuang-zhi, JIANG Chang-yi, et al. Trends of Research in Exploration of Magmatic Sulfide Deposits and Small Intrusions Metallogenic System[J]. Journal of Earth Sciences and Environment, 2011, 33(1): 1-9.

[4] **宋谢炎,张成江,胡瑞忠,等.峨眉火成岩省岩浆矿床成矿作用与地幔柱动力学过程的耦合关系**[J].**矿物岩石**,2005,25(4):35-44.
SONG Xie-yan, ZHANG Cheng-jiang, HU Rui-zhong, et al. Genetic Links of Magmatic Deposits in the Emeishan Large Igneous Province with Dynamics of Mantle Plume[J]. Journal of Mineralogy and Petrology, 2005, 25(4): 35-44.

[5] **焦建刚,汤中立,钱壮志,等.东天山地区图拉尔根铜镍硫化物矿床成因及成矿过程**[J].**岩石学报**,2012,28(11):3772-3786.
JIAO Jian-gang, TANG Zhong-li, QIAN Zhuang-zhi, et al. Genesis and Metallogenic Process of Tulargen Large Scale Cu-Ni Sulfide Deposit in Eastern Tianshan Area, Xinjiang[J]. Acta Petrologica Sinica, 2012, 28(11): 3772-3786.

[6] RIPLEY E M, LI C. Sulfide Saturation in Mafic Magmas: Is External Sulfur Required for Magmatic Ni-Cu-(PGE) Ore Genesis?[J]. Economic Geology, 2013, 108(1): 45-58.

[7] YANG S H, ZHOU M F, LIGHTFOOT P C, et al. Re-Os Isotope and Platinum-group Element Geochemistry of the Pobei Ni-Cu Sulfide-bearing Mafic-ultramafic Complex in the Northeastern Part of the Tarim Craton[J]. Mineralium Deposita, 2014, 49(3): 381-397.

[8] HOLWELL D A, MITCHELL C L, HOWE G A, et al. The Munali Ni Sulfide Deposit, Southern Zambia: A Multi-stage, Mafic-ultramafic, Magmatic Sulfide-magnetite-apatite-carbonate Megabreccia[J]. Ore Geology Reviews, 2017, 90: 553-575.

[9] KANG J, WILLE M, HOFMANN B A, et al. Heterogeneous Lead Isotopic Compositions of Sulfide Minerals from a Hydrothermal Replacement Deposit(Janggun Mine, South Korea)[J]. Ore Geology Reviews, 2020, 122: 103527.

[10] **孙　涛,钱壮志,党新生,等.喀拉通克铜镍矿床硫同位素组成特征及其地质意义**[J].**地球科学与环境学报**,2010,32(4):344-349.
SUN Tao, QIAN Zhuang-zhi, DANG Xin-sheng, et al. Characteristics of Sulfur Isotope in Kalatongke Cu-Ni Deposit and Its Geological Significance[J]. Journal of Earth Sciences and Environment, 2010, 32(4): 344-349.

[11] **宫　丽,马　光.黄铁矿的成分标型特征及其在金属矿床中的指示意义**[J].**地质找矿论丛**,2011,26(2):162-166.
GONG Li, MA Guang. The Characteristic Typomorphic Composition of Pyrite and Its Indicative Meaning to Metal Deposits[J]. Contributions to Geology and Mineral Resources Research, 2011, 26(2): 162-166.

[12] **曾　茜,陈守余,赵江南.个旧锡矿东区黄铁矿成分标型特征研究**[J].**地质找矿论丛**,2017,32(3):375-384.
ZENG Xi, CHEN Shou-yu, ZHAO Jiang-nan. Composition Typomorphic Characteristics of Pyrite in East Part of Gejiu[J]. Contributions to Geology and Mineral Resources Research, 2017, 32(3): 375-384.

[13] **王冬丽,申俊峰,邱海成,等.辽宁五龙金矿黄铁矿标型特征研究及深部找矿预测**[J].**南京大学学报(自然科学)**,2019,55(6):898-915.
WANG Dong-li, SHEN Jun-feng, QIU Hai-cheng, et al. Study on Typomorphic Characteristics of Pyrite and Prediction of Deep Prospecting of Wulong Gold Deposit in Liaoning Province[J]. Journal of Nanjing University(Natural Science), 2019, 55(6): 898-915.

[14] **李洪梁,李光明.不同类型热液金矿床主成矿期黄铁矿成分标型特征**[J].**地学前缘**,2019,26(3):202-210.
LI Hong-liang, LI Guang-ming. Compositional Characteristics of Pyrite Ore Formed in the Main Metallogenic Period of Various Types of Hydrothermal Gold Deposits[J]. Earth Science Frontiers, 2019, 26(3): 202-210.

[15] **严千豪,王翠芝,吕古贤,等.胶东玲珑金矿黄铁矿的化学成分标型特征及其矿床学意义**[J].**地质找矿论丛**,2020,35(1):52-63.
YAN Qian-hao, WANG Cui-zhi, LYU Gu-xian, et al. Typomorphic Characteristics of Chemical Composi-

tion of Pyrite and Its Significance in Linglong Gold Deposit, Jiaodong Peninsula[J]. Contributions to Geology and Mineral Resources Research, 2020, 35(1): 52-63.

[16] 尤敏鑫，张照伟，刘建民，等. 攀西地区镁铁—超镁铁岩地球化学与岩浆型 Cu-Ni-(PGE)硫化物矿床成矿[J]. 西北地质，2017，50(3)：146-161.
YOU Min-xin, ZHANG Zhao-wei, LIU Jian-min, et al. Geochemistry of Mafic-ultramafic Intrusions and Cu-Ni-(PGE) Sulfide Deposits in Panxi Region, China [J]. Northwestern Geology, 2017, 50(3): 146-161.

[17] DING X, RIPLEY E M, WANG W Z, et al. Iron Isotope Fractionation During Sulfide Liquid Segregation and Crystallization at the Lengshuiqing Ni-Cu Magmatic Sulfide Deposit, SW China[J]. Geochimica et Cosmochimica Acta, 2019, 261: 327-341.

[18] 卢宜冠，和文言. 滇西金宝山铂钯矿床 S-Os 同位素特征及其对成矿过程的制约[J]. 岩石学报，2018，34(5)：1258-1270.
LU Yi-guan, HE Wen-yan. Characteristics of S-Os Isotopes and Its Constraints on the Mineralization for the Jinbaoshan Pt-Pd Deposit, Western Yunnan, China [J]. Acta Petrologica Sinica, 2018, 34(5): 1258-1270.

[19] LIANG Q L, SONG X Y, WIRTH R, et al. Implications of Nano- and Micrometer-size Platinum-group Element Minerals in Base Metal Sulfides of the Yangliuping Ni-Cu-PGE Sulfide Deposit, SW China[J]. Chemical Geology, 2019, 517: 7-21.

[20] 王生伟，孙晓明，廖震文，等. 云南金宝山铂钯矿床铂族元素地球化学及找矿意义[J]. 矿床地质，2012，31(6)：1259-1276.
WANG Sheng-wei, SUN Xiao-ming, LIAO Zhen-wen, et al. Platinum Group Elements Geochemistry of Jinbaoshan Pt-Pd Deposit in Yunnan Province and Its Exploration Implications[J]. Mineral Deposits, 2012, 31(6): 1259-1276.

[21] 马言胜，陶　琰，朱　丹，等. 云南朱布镁铁—超镁铁岩体地球化学特征及成因机理探讨[J]. 地球化学，2012，41(4)：359-370.
MA Yan-sheng, TAO Yan, ZHU Dan, et al. Geochemical Characteristics and Genesis of the Zhubu Mafic-ultramafic Intrusion, Yunnan Province [J]. Geochimica, 2012, 41(4): 359-370.

[22] 高　媛. 四川省丹巴县杨柳坪 Ni-PGE 矿床岩矿特征及 PGE 赋存状态的研究[D]. 成都：成都理工大学，2011.
GAO Yuan. Petrology, Ore Characteristics and the Occurrence of PGE in Yangliuping Ni-PGE Deposit, Danba Sichuan[D]. Chengdu: Chengdu University of Technology, 2011.

[23] 李永生，张招崇. 能量约束下的同化混染与分离结晶作用模型(EC-AFC)在超镁铁质岩浆演化过程中的应用：以含铜镍硫化物矿床的四川力马河岩体为例[J]. 岩石学报，2011，27(10)：2975-2983.
LI Yong-sheng, ZHANG Zhao-chong. Application of Energy-constrained Assimilation-fractional Crystallization (EC-AFC) Model for Ultramafic Magmatic Systems: A Case Study of the Limahe Intrusion Associated with Cu-Ni Sulfide Ores, Sichuan Province[J]. Acta Petrologica Sinica, 2011, 27(10): 2975-2983.

[24] 戚学祥，朱路华，李志群. 哀牢山—金沙江构造带白马寨铜镍硫化物矿床Ⅰ号含矿岩体铂族元素地球化学特征及其构造意义[J]. 现代地质，2010，24(1)：98-106.
QI Xue-xiang, ZHU Lu-hua, LI Zhi-qun. Platinum Group Elements (PGE) Geochemistry of the Ore-bearing Intrusive Body Ⅰ from the Baimazhai Cu-Ni Deposit in the Ailaoshan-Jinshajiang Tectonic Zone and Its Significance[J]. Geoscience, 2010, 24(1): 98-106.

[25] 苟体忠，钟　宏，朱维光，等. 川西冷水箐 Cu-Ni 硫化物矿床的 PGE 和 Re-Os 同位素地球化学特征及成矿意义[J]. 岩石学报，2010，26(11)：3363-3374.
GOU Ti-zhong, ZHONG Hong, ZHU Wei-guang, et al. Geochemical Characteristics of Platinum-group Elements and Re-Os Isotope of the Lengshuiqing Cu-Ni Sulfide Deposit in Western Sichuan Province and Implications for Mineralization[J]. Acta Petrologica Sinica, 2010, 26(11): 3363-3374.

[26] 马言胜，陶　琰，朱飞霖，等. 金宝山铂-钯矿和力马河镍矿的硫同位素组成特征及地质意义[J]. 矿物岩石地球化学通报，2009，28(2)：123-127.
MA Yan-sheng, TAO Yan, ZHU Fei-lin, et al. The Sulfur Isotopic Characteristics and Geological Significance of Jinbaoshan Pt-Pd Deposit and Limahe Nickel Deposit [J]. Bulletin of Mineralogy, Petrology and Geochemistry, 2009, 28(2): 123-127.

[27] ZHANG Z C, HAO Y L, YU A I, et al. Phase Equilibria Constraints on Relations of Ore-bearing Intrusions with Flood Basalts in the Panxi Region, Southwestern China[J]. Acta Geologica Sinica (English Edition), 2009, 83(2): 111-125.

[28] 陶　琰，胡瑞忠，屈文俊，等. 力马河镍矿 Re-Os 同位素研究[J]. 地质学报，2008，82(9)：1292-1304.
TAO Yan, HU Rui-zhong, QU Wen-jun, et al. Re-Os Isotope Study of Sulfide and Olivine Pyroxenite in the Limahe Nickle Deposit, Sichuan Province [J]. Acta

Geologica Sinica,2008,82(9):1292-1304.

[29] 王 焰.云南二叠纪白马寨铜镍硫化物矿床的成因:地壳混染与矿化的关系[J].矿物岩石地球化学通报,2008,27(4):332-343.
WANG Yan. Origin of the Permian Baimazhai Magmatic Ni-Cu-(PGE) Sulfide Deposits, Yunnan: Implications for the Relationship of Crustal Contamination and Mineralization[J]. Bulletin of Mineralogy, Petrology and Geochemistry,2008,27(4):332-343.

[30] 孙晓明,王生伟,石贵勇,等.云南白马寨 Cu-Ni 硫化物矿微量和铂族元素地球化学和矿床成因意义[J].矿物岩石地球化学通报,2008,27(3):239-246.
SUN Xiao-ming, WANG Sheng-wei, SHI Gui-yong, et al. Trace and Platinum Group Elements (PGE) Geochemistry of Sulfide Ores and Related Intrusive Rocks from the Baimazhai Cu-Ni Deposit in Yunnan Province, China[J]. Bulletin of Mineralogy, Petrology and Geochemistry,2008,27(3):239-246.

[31] 宋谢炎,曹志敏,罗辅勋,等.四川丹巴杨柳坪铜镍铂族元素硫化物矿床成因初探[J].成都理工大学学报(自然科学版),2004,31(3):256-266.
SONG Xie-yan, CAO Zhi-min, LUO Fu-xun, et al. Origin of Yangliuping Ni-Cu-PGE Sulfide Deposit in Danba, Sichuan[J]. Journal of Chengdu University of Technology (Science and Technology Edition),2004,31(3):256-266.

[32] 李文渊,王亚磊,钱 兵,等.塔里木陆块周缘岩浆 Cu-Ni-Co 硫化物矿床形成的探讨[J].地学前缘,2020,27(2):276-293.
LI Wen-yuan, WANG Ya-lei, QIAN Bing, et al. Discussion on the Formation of Magmatic Cu-Ni-Co Sulfide Deposits in Margin of Tarim Block[J]. Earth Science Frontiers,2020,27(2):276-293.

[33] 王登红,骆耀南,傅德明,等.四川杨柳坪 Cu-Ni-PGE 矿区基性—超基性岩的地球化学特征及其含矿性[J].地球学报,2001,22(2):135-140.
WANG Deng-hong, LUO Yao-nan, FU De-ming, et al. Petrochemistry and Ore Potentiality of the Mafic-ultramafic Rocks in the Yangliuping Cu-Ni-PGE Mine, Sichuan Province[J]. Acta Geoscientica Sinica,2001,22(2):135-140.

[34] ZHOU M F, ARNDT N T, MALPAS J, et al. Two Magma Series and Associated Ore Deposit Types in the Permian Emeishan Large Igneous Province, SW China[J]. Lithos,2008,103(3):352-368.

[35] SONG X Y, ZHOU M F, TAO Y, et al. Controls on the Metal Compositions of Magmatic Sulfide Deposits in the Emeishan Large Igneous Province, SW China [J]. Chemical Geology,2008,253(1):38-49.

[36] 宋谢炎.岩浆硫化物矿床研究现状及重要科学问题[J].矿床地质,2019,38(4):699-710.
SONG Xie-yan. Current Research Status and Important Issues of Magmatic Sulfide Deposits[J]. Mineral Deposits,2019,38(4):699-710.

[37] 张晓荔.攀西地区含矿基性—超基性岩岩石地球化学特征及成矿作用分析[D].成都:成都理工大学,2015.
ZHANG Xiao-li. The Petrogeochemical Characteristics and the Metallogenic Analysis of the Ore-bearing Basic-ultrabasic Rocks in Panxi, Sichuan[D]. Chengdu: Chengdu University of Technology,2015.

[38] 李浩然.攀西地区基性—超基性岩岩石地球化学特征及岩浆演化过程分析[D].成都:成都理工大学,2015.
LI Hao-ran. The Lithogeochemical Characteristics and Magma Evolution of the Mafic-ultramafic Intrusions in Panxi District[D]. Chengdu: Chengdu University of Technology,2015.

[39] 任光明,李佑国,陈 旭,等.攀西地区铂族元素地球化学异常分布及其筛选[J].地质与勘探,2008,44(1):62-66.
REN Guang-ming, LI You-guo, CHEN Xu, et al. Distribution and Sieving of Geochemical Anomalies of PG Elements in the Panxi Region[J]. Geology and Prospecting,2008,44(1):62-66.

[40] 张招崇,李 莹,赵 莉,等.攀西三个镁铁—超镁铁质岩体的地球化学及其对源区的约束[J].岩石学报,2007,23(10):2339-2352.
ZHANG Zhao-chong, LI Ying, ZHAO Li, et al. Geochemistry of Three Layered Mafic-ultramafic Intrusions in the Panxi Area and Constraints on Their Sources[J]. Acta Petrologica Sinica,2007,23(10):2339-2352.

[41] 傅敏军.攀西红格钒钛磁铁矿床地质特征及控矿因素分析[D].成都:成都理工大学,2012.
FU Min-jun. Analysis on Geological Characteristics and Ore-controlling Factors of Vanadium Titano-magnetite Deposits in Hongge, Pan-Xi [D]. Chengdu: Chengdu University of Technology,2012.

[42] 徐国风,邵洁涟.黄铁矿的标型特征及其实际意义[J].地质论评,1980,26(6):541-546.
XU Guo-feng, SHAO Jie-lian. The Typomorphic Characteristics of Pyrite and Its Significance[J]. Geological Review,1980,26(6):541-546.

[43] 柯昌辉,吕新彪,王玉奇,等.河南省罗山县金城金矿黄铁矿标型特征及其意义[J].岩石矿物学杂志,

2012,31(2):225-234.
KE Chang-hui,LU Xin-biao,WANG Yu-qi,et al. Typomorphic Features and Exploration Significance of Pyrite from the Jincheng Gold Deposit in Luoshan, Henan Province[J]. Acta Petrologica et Mineralogica, 2012,31(2):225-234.

[44] 封兴福,王建国. 四川省渡口市红格含钒钛磁铁矿基性—超基性岩体地质普查报告[R]. 成都:四川省地质局攀西地质队二区队,1982.
FENG Xing-fu, WANG Jian-guo. Geological Survey Report on Basic-ultrabasic Rock Mass of Hongge Vanadium Bearing Titano-magnetite in Dukou City, Sichuan Province[R]. Chengdu: No. 2 Division of Panxi Geological Brigade,Sichuan Bureau of Geology,1982.

[45] 何　益. 攀枝花层状岩体钪的地球化学特征及富集规律[D]. 成都:成都理工大学,2016.
HE Yi. The Geochemical Features and Concentration Regularity of Scandium in Stratified Rock Mass of Panzhihua[D]. Chengdu:Chengdu University of Technology,2016.

[46] 严育通,李胜荣,贾宝剑,等. 中国不同成因类型金矿床的黄铁矿成分标型特征及统计分析[J]. 地学前缘, 2012,19(4):214-226.
YAN Yu-tong, LI Sheng-rong, JIA Bao-jian, et al. Composition Typomorphic Characteristics and Statistic Analysis of Pyrite in Gold Deposits of Different Genetic Types[J]. Earth Science Frontiers, 2012, 19 (4):214-226.

[47] 要梅娟. 南非布什维尔德铂族矿床中铂族金属富集机理研究[D]. 北京:中国地质大学,2012.
YAO Mei-juan. Enrichment Mechanism of Platinum Group Metals, Bushveld PGE Deposits, South Africa [D]. Beijing:China University of Geosciences,2012.

[48] BAILEY J,MCDONALD A M,LAFRANCE B,et al. Variations in Ni Content in Sheared Magmatic Sulfide Ore at the Thayer Lindsley Mine, Sudbury, Ontario [J]. The Canadian Mineralogist, 2006, 44(5): 1063-1077.

[49] 陈　亮. 甘肃金川铜镍硫化物矿床金属硫化物矿物学特征研究[D]. 北京:中国地质大学,2008.
CHEN Liang. Study on the Mineralogy Characteristics of Metallic Sulphide in the Jinchuan Ni-Cu Sulfide Ore Deposit,Gansu Province[D]. Beijing: China University of Geosciences,2008.

[50] 宋忠宝,姜常义,凌锦兰,等. 青海省基性超基性岩与岩浆型铜镍硫化物矿床[M]. 北京: 地质出版社, 2015.
SONG Zhong-bao, JIANG Chang-yi, LING Jin-lan, et al. Petrogenesis of Mafic-ultramafic Intrusions and Minerogenesis of Cu-Ni Sulfide Deposit in Qinghai Province[M]. Beijing: Geological Publishing House, 2015.

[51] 吕林素,李宏博,周振华,等. 吉林红旗岭富家矿床矿石矿物化学和硫同位素特征:对铜镍硫化物矿床成因及成矿过程的约束[J]. 地球学报,2017,38(2):193-207.
LU Lin-su, LI Hong-bo, ZHOU Zhen-hua, et al. Mineral Chemistry and Sulfur Isotopic Characteristics of Ores from the Fujia Deposit in Hongqiling Area, Jilin Province: Constraints on the Genesis and Ore-forming Processes of Ni-Cu Sulfide Deposit[J]. Acta Geoscientica Sinica,2017,38(2):193-207.

[52] 郗爱华,任洪茂,张宝福,等. 吉林省红旗岭铜镍硫化物矿床矿石学特征[J]. 吉林大学学报(地球科学版), 2004,34(3):338-343.
XI Ai-hua, REN Hong-mao, ZHANG Bao-fu, et al. Characteristics on Ore Minerals in Hongqiling Cu-Ni Sulfide Deposit, Jilin Province[J]. Journal of Jilin University(Earth Science Edition), 2004, 34(3): 338-343.

[53] 赵玉梅. 新疆喀拉通克铜镍矿床矿石矿物微区分析[D]. 西安:长安大学,2009.
ZHAO Yu-mei. Microregion Analyse of the Ore Minerals of Kalatongke Nickel-copper Deposit, Xinjiang [D]. Xi'an:Chang'an University,2009.

[54] 王建中. 新疆喀拉通克铜镍硫化物矿床成矿作用与成矿潜力研究[D]. 西安:长安大学,2010.
WANG Jian-zhong. The Minerogenesis and Metallogenic Potential of Kalatongke Nickel-copper Sulfide Deposit, Xinjiang, China[D]. Xi'an: Chang'an University,2010.

[55] 李烁隐. 陕西煎茶岭镍矿床超基性岩矿物学研究[D]. 北京:中国地质大学,2019.
LI Shuo-yin. Mineralogy Study of Ultrabasic Rocks in the Nickel Deposit of Jianchaling, Shaanxi Province [D]. Beijing:China University of Geosciences,2019.

[56] 王志华,侯　岚,高永伟,等. 西天山智博铁矿床黄铁矿成分特征及硫同位素研究[J]. 矿床地质,2018,37(6):1319-1336.
WANG Zhi-hua, HOU Lan, GAO Yong-wei, et al. Chemical Composition and Sulfur Isotope of Pyrite from Zhibo Iron Ore Deposit in Western Tianshan Mountains[J]. Mineral Deposits, 2018, 37(6): 1319-1336.

[57] 陈光远,孙岱生,殷辉安. 成因矿物学与找矿矿物学[M]. 重庆:重庆出版社,1988.

CHEN Guang-yuan, SUN Dai-sheng, YIN Hui-an. Genetic Mineralogy and Prospecting Mineralogy[M]. Chongqing: Chongqing Publishing House, 1988.

[58] BRILL B A. Trace-element Contents and Partitioning of Elements in Ore Minerals from the CSA Cu-Pb-Zn Deposit, Australia[J]. The Canadian Mineralogist, 1989, 27(7): 263-274.

[59] CLARK C, GRGURIC B, MUMM A S. Genetic Implications of Pyrite Chemistry from the Palaeoproterozoic Olary Domain and Overlying Neoproterozoic Adelaidean Sequences, Northeastern South Australia[J]. Ore Geology Reviews, 2004, 25(3): 237-257.

[60] **王奎仁. 地球与宇宙成因矿物学**[M]. **合肥:安徽教育出版社**, 1989.
WANG Kui-ren. Genetic Mineralogy of Earth and Universe[M]. Hefei: Anhui Education Press, 1989.

[61] ZHOU J X, HUANG Z L, ZHOU G F, et al. Trace Elements and Rare Earth Elements of Sulfide Minerals in the Tianqiao Pb-Zn Ore Deposit, Guizhou Province, China[J]. Acta Geologica Sinica (English Edition), 2011, 85(1): 189-199.

[62] **涂光炽, 刘英俊, 赵振华, 等. 矿床地球化学**[M]. **北京:地质出版社**, 1997.
TU Guang-chi, LIU Ying-jun, ZHAO Zhen-hua, et al. Geochemistry of Ore Deposit[M]. Beijing: Geological Publishing House, 1997.

[63] **杨喜安, 刘家军, 韩思宇, 等. 云南羊拉铜矿床矿物组成、地球化学特征及其地质意义**[J]. **现代地质**, 2012, 26(2): 229-242.
YANG Xi-an, LIU Jia-jun, HAN Si-yu, et al. Mineral Composition, Geochemistry of the Yangla Copper Deposit in Yunnan and Their Geological Significances[J]. Geoscience, 2012, 26(2): 229-242.

[64] **靳是琴, 李鸿超. 成因矿物学概论**[M]. **长春:吉林大学出版社**, 1984.
JIN Shi-qin, LI Hong-chao. An Introduction to Genetic Mineralogy[M]. Changchun: Jilin University Press, 1984.

[65] **刘英俊, 曹励明, 李兆麟, 等. 元素地球化学**[M]. **北京:科学出版社**, 1984.
LIU Ying-jun, CAO Li-ming, LI Zhao-lin, et al. Geochemistry of Element[M]. Beijing: Science Press, 1984.

[66] RIPLEY E M. Se/S Ratios of the Virginia Formation and Cu-Ni Sulfide Mineralization in the Babbitt Area, Duluth Complex, Minnesota[J]. Economic Geology, 1990, 85(8): 1935-1940.

[67] RIPLEY E M, LI C, SHIN D. Paragneiss Assimilation in the Genesis of Magmatic Ni-Cu-Co Sulfide Mineralization at Voisey's Bay, Labrador: $\delta^{34}S$, $\delta^{13}C$, and Se/S Evidence[J]. Economic Geology, 2002, 97(6): 1307-1318.

[68] **李胜荣. 结晶学与矿物学**[M]. **北京:地质出版社**, 2008.
LI Sheng-rong. Crystallography and Mineralogy[M]. Beijing: Geological Publishing House, 2008.

[69] BAJWAH Z U, SECCOMBE P K, OFFLER R. Trace Element Distribution, Co:Ni Ratios and Genesis of the Big Cadia Iron-copper Deposit, New South Wales, Australia[J]. Mineralium Deposita, 1987, 22(4): 292-300.

[70] **毛光周, 华仁民, 高剑峰, 等. 江西金山金矿床含金黄铁矿的稀土元素和微量元素特征**[J]. **矿床地质**, 2006, 25(4): 412-426.
MAO Guang-zhou, HUA Ren-min, GAO Jian-feng, et al. REE Composition and Trace Element Features of Gold-bearing Pyrite in Jinshan Gold Deposit, Jiangxi Province[J]. Mineral Deposits, 2006, 25(4): 412-426.

[71] **黎 彤, 倪守斌. 地球和地壳的化学元素丰度**[M]. **北京:地质出版社**, 1990.
LI Tong, NI Shou-bin. The Abundance of Chemical Elements in Earth and Its Crust[M]. Beijing: Geological Publishing House, 1990.

[72] **李成禄, 李胜荣, 袁茂文, 等. 黑龙江省嫩江—黑河构造混杂岩带科洛金矿床成因:来自黄铁矿化学成分及 He-Ar、S、Pb 同位素证据**[J]. **地学前缘**, 2020, 27(5): 99-115.
LI Cheng-lu, LI Sheng-rong, YUAN Mao-wen, et al. Genesis of the Keluo Au Deposit in the Nenjiang-Heihe Tectonic Melange Belt, Heilongjiang Province: Evidence from Chemical Composition and Pyrite He-Ar, S, Pb Isotopes[J]. Earth Science Frontiers, 2020, 27(5): 99-115.

[73] **何阳阳, 温春齐, 刘显凡. 西藏多不杂铜矿床黄铁矿成分标型特征及地质意义**[J]. **地质找矿论丛**, 2019, 34(3): 432-437.
HE Yang-yang, WEN Chun-qi, LIU Xian-fan. Typomorphic Characteristics of the Pyrite Composition in the Duobuza Copper Deposit, Tibet and the Geological Significance[J]. Contributions to Geology and Mineral Resources Research, 2019, 34(3): 432-437.

[74] MCDONOUGH W F, SUN S S. The Composition of the Earth[J]. Chemical Geology, 1995, 120(3): 223-253.

[75] **宋谢炎, 陈列锰, 于宋月, 等. 峨眉大火成岩省钒钛磁铁矿矿床地质特征及成因**[J]. **矿物岩石地球化学通报**, 2018, 37(6): 1003-1018.

SONG Xie-yan, CHEN Lie-meng, YU Song-yue, et al. Geological Features and Genesis of the V-Ti Magenetite Deposits in the Emeishan Large Igneous Province, SW China[J]. Bulletin of Mineralogy, Petrology and Geochemistry, 2018, 37(6): 1003-1018.

[76] 钟　祥，郗爱华，葛玉辉，等. 攀西白马岩体的矿物结晶顺序与钒钛磁铁矿成因[J]. 矿物学报，2018，38(4)：449-461.
ZHONG Xiang, XI Ai-hua, GE YU-hui, et al. Crystallization Sequence of Minerals and Origin of the Fe-Ti-V Oxide Ores from the Baima Layered Intrusion in the Panxi Area[J]. Acta Mineralogica Sinica, 2018, 38(4): 449-461.

[77] 郝江波，刘严松，何政伟，等. 攀西地区红格钒钛磁铁矿床地球化学异常特征分析及矿床成因探讨[J]. 西北地质，2016，49(1)：206-213.
HAO Jiang-bo, LIU Yan-song, HE Zheng-wei, et al. Geochemical Anomaly Characteristics and Genesis of the Hongge Vanadic Titano-magnetite Deposit in Panzhihua-Xichang Region[J]. Northwestern Geology, 2016, 49(1): 206-213.

[78] 栾　燕，宋谢炎，陈列锰，等. 四川红格层状侵入体中角闪石和金云母的矿物学特征及其成因意义[J]. 岩石学报，2014，30(5)：1457-1471.
LUAN Yan, SONG Xie-yan, CHEN Lie-meng, et al. Mineralogical Features and Petrogenetic Significances of the Hornblende and Phlogopite of the Hongge Layered Intrusion, Sichuan Province[J]. Acta Petrologica Sinica, 2014, 30(5): 1457-1471.

[79] 佘宇伟，宋谢炎，于宋月，等. 磁铁矿和钛铁矿成分对四川太和富磷灰石钒钛磁铁矿床成因的约束[J]. 岩石学报，2014，30(5)：1443-1456.
SHE Yu-wei, SONG Xie-yan, YU Song-yue, et al. The Compositions of Magnetite and Ilmenite of the Taihe Layered Intrusion, Sichuan Province: Constraints on the Formation of the P-rich Fe-Ti Oxide Ores[J]. Acta Petrologica Sinica, 2014, 30(5): 1443-1456.

[80] HOU T, ZHANG Z C, ENCARNACION J, et al. Petrogenesis and Metallogenesis of the Taihe Gabbroic Intrusion Associated with Fe-Ti-oxide Ores in the Panxi District, Emeishan Large Igneous Province, Southwest China[J]. Ore Geology Reviews, 2012, 49: 109-127.

[81] 王世霞，朱祥坤，宋谢炎，等. 四川攀枝花钒钛磁铁矿床 Fe 同位素特征及其成因指示意义[J]. 地球学报，2012，33(6)：995-1004.
WANG Shi-xia, ZHU Xiang-kun, SONG Xie-yan, et al. Fe Isotopic Characteristics of V-Ti Magnetite Deposit in Panzhihua Area of Sichuan Province and Their Genetic Implications[J]. Acta Geoscientica Sinica, 2012, 33(6): 995-1004.

[82] SHELLNUTT J G, WANG K L, ZELLMER G F, et al. Three Fe-Ti Oxide Ore-bearing Gabbro-granitoid Complexes in the Panxi Region of the Permian Emeishan Large Igneous Province, SW China[J]. American Journal of Science, 2011, 311(9): 773-812.

[83] 张晓琪，张加飞，宋谢炎，等. 斜长石和橄榄石成分对四川攀枝花钒钛磁铁矿床成因的指示意义[J]. 岩石学报，2011，27(12)：3675-3688.
ZHANG Xiao-qi, ZHANG Jia-fei, SONG Xie-yan, et al. Implications of Compositions of Plagioclase and Olivine on the Formation of the Panzhihua V-Ti Magnetite Deposit, Sichuan Province[J]. Acta Petrologica Sinica, 2011, 27(12): 3675-3688.

[84] XU J F, SUZUKI K, XU Y G, et al. Os, Pb, and Nd Isotope Geochemistry of the Permian Emeishan Continental Flood Basalts: Insights into the Source of a Large Igneous Province[J]. Geochimica et Cosmochimica Acta, 2007, 71(8): 2104-2119.

[85] 周美夫. 攀西地区层状辉长岩体及钒钛磁铁矿床的成因[J]. 岩石矿物学杂志，2005，24(5)：381-384.
ZHOU Mei-fu. Origin of Layered Gabbroic Intrusions and Their Giant Fe-Ti-V Oxide Deposits in the Pan-Xi District, Sichuan Province, SW China[J]. Acta Petrologica et Mineralogica, 2005, 24(5): 381-384.

[86] XU Y G, CHUNG S L, JAHN B M, et al. Petrologic and Geochemical Constraints on the Petrogenesis of Permian-Triassic Emeishan Flood Basalts in Southwestern China[J]. Lithos, 2001, 58(3/4): 145-168.

[87] 王汾连，赵太平，王　焰. 攀西地区二叠纪赋存铌钽矿的正长岩脉的成因探讨[J]. 岩石学报，2015，31(6)：1797-1805.
WANG Fen-lian, ZHAO Tai-ping, WANG Yan. Petrogenisis of Permian Nb-Ta Mineralized Syenitic Dikes in the Panxi District, SW China[J]. Acta Petrologica Sinica, 2015, 31(6): 1797-1805.